arXiv:1612.09053v1 [cond-mat.supr-con] 29 Dec 2016

Covariant gaussian approximation in Ginzburg - Landau model

J.F. Wang[a,b], D.P. Li[a,b], H.C. Kao[c], B. Rosenstein[d]

[a]*School of Physics, Peking University, Beijing 100871, China*
[b]*Collaborative Innovation Center of Quantum Matter, Beijing 100871, China*
[c]*Physics Department, National Taiwan Normal University, Taipei 11677, Taiwan, R.O.C.*
[d]*Electrophysics Department, National Chiao Tung University, Hsinchu 30050, Taiwan, R.O.C.*

Abstract

Condensed matter systems undergoing second order transition away from the critical fluctuation region are usually described sufficiently well by the mean field approximation. The critical fluctuation region, determined by the Ginzburg criterion, $|T/T_c - 1| \ll Gi$, is narrow even in high T_c superconductors and has universal features well captured by the renormalization group method. However recent experiments on magnetization, conductivity and Nernst effect suggest that fluctuations effects are large in a wider region both above and below T_c. In particular some "pseudogap" phenomena and strong renormalization of the mean field critical temperature T_{mf} can be interpreted as strong fluctuations effects that are nonperturbative (cannot be accounted for by "gaussian fluctuations"). The physics in a broader region therefore requires more accurate approach. Self consistent methods are generally "non - conserving" in the sense that the Ward identities are not obeyed. This is especially detrimental in the symmetry broken phase where, for example, Goldstone bosons become massive. Covariant gaussian approximation remedies these problems. The Green's functions obey all the Ward identities and describe the fluctuations much better. The results for the order parameter correlator and magnetic penetration depth of the Ginzburg - Landau model of superconductivity are compared with both Monte Carlo simulations and experiments in high T_c cuprates.

Keywords: Covariant gaussian approximation, Ginzburg - Landau, Ward identity, superconducting thermal fluctuations, magnetic penetration depth

1. Introduction

Many - body systems at nonzero temperature exhibit a host of physical phenomena triggered by strong thermal fluctuations[1]. Most remarkable are of course phase transitions, in which the ground state rearranges. In addition, crossovers and qualitatively recognizable phenomena, such as metastability or possibly the "pseudogap" physics in high T_c cuprates, also attract intensive interest. It was noticed by Landau that for temperatures close to critical point of a second order transition, symmetry and energetics considerations suggest that the system can be described by a rather simple universal Ginzburg - Landau (GL) model. The model expressed in terms of an appropriate order parameter field ϕ contains a very small number of phenomenological parameters, since one retains only terms up to fourth power of ϕ in the GL free energy (on the condition that it is well separated from the tricritical point where the sixth order of ϕ cannot be neglected).

The universality was established in the critical fluctuation region, where physics is determined by several critical exponents well captured by the renormalization group approach to the GL ϕ^4 theory[2]. However the width of the critical region, determined by the Ginzburg criterion[3], $|T/T_c - 1| \ll Gi$, is very narrow even in the most fluctuating materials like the high T_c superconductors for which the Ginzburg number Gi is of order 0.05. Away from the critical fluctuation region, the universality might not hold. One thus traditionally resorts to a variety of mean field or self - consistent models. These models focus on different degrees of freedom, and so a statistical system is often represented in several different ways depending on the choice of the quantity that is considered self - consistently. Examples of self - consistent approaches range from the Bragg - Williams approximation for spin systems to the BCS approximation of conventional superconductors and the Hartree - Fock approximation in the electron gas or liquid. Thus the mean field approach is essentially different from the economic GL description in terms of the order parameter field ϕ defined

solely by the symmetry properties of the system. A question arises whether the GL model can nevertheless be reliable away from its intended range of applicability near the criticality.

The GL approach in terms of the order parameter however is in fact widely and successfully used for description of the fluctuations outside the critical region[4]. There are several arguments why actually one can use the universal model beyond its original range of applicability[1, 3, 5]. Very often the fluctuations are accounted for by the gaussian fluctuations approximation to the GL model[6]. This completely neglects the ϕ^4 coupling of the order parameter that sometimes is included perturbatively[3]. Various approximations beyond perturbation theory were developed.

Recent experiments on magnetization[7], conductivity[8] and Nernst effect[9] of high T_c superconductors suggest that fluctuation effects are significant and even large in a much wider region both above and below T_c. First of all, the renormalization of the critical temperature T_c from its "microscopic" or "mean field" value, T_{mf}, is non - universal and might be of the same order of magnitude as T_c. Superconducting fluctuations as far above T_c as $2T_c$ still dominate over the normal state contributions to the above three physical phenomena. Similarly below T_c (sometimes even close to zero temperature and definitely far away from the critical fluctuation region) the fluctuations determine the nontrivial penetration depth dependence on temperature[10, 11, 12] and magnetic properties[4]. In particular some of the still poorly understood phenomena in underdoped and optimally doped cuprates known as the "pseudogap" features[13] can be interpreted as strong fluctuations effects that are nonperturbative[14] (cannot be accounted for by gaussian fluctuations) rather than stemming from a yet unknown microscopic origin.

It has been noted over the years that despite the anticipated breakdown of the universality far beyond the critical fluctuation region strong fluctuations are still well captured by the interacting ϕ^4 GL theory[3, 4]. Of course some approximations have to be made and the most natural is a self - consistent method for the expectation value and the correlator of the order parameter field known as gaussian approximation[15]. As in most of the standard variants of the self - consistent mean field theories, within the gaussian approximation one encounters a difficulty with preserving the basic symmetries of the problem. In the symmetric phase gaussian approximation (mean field in terms of the order parameter and its correlator) is generally symmetry conserving and thus sufficient for qualitative and even quantitative description. However below the transition temperature this is not the case. The symmetry is not preserved within the "naive" gaussian approximation and as a result even such a basic phenomenon as appearance of massless Goldstone modes in the symmetry broken phase cannot be accounted for. The excitation becomes massive and thus a symmetry conserving approach is required[16].

In this paper we show that a special uniquely defined variant of the mean field approximation, the covariant gaussian approximation (CGA) around the spontaneous symmetry broken state satisfies this requirement. The approximation is conserving in that it preserves the symmetry properties of the correlators of the order parameter characterizing the ordered phase. The CGA Green's functions obey all the Ward identities and describe the fluctuations much better. The results for the two and four point correlators of the Ginzburg - Landau model are compared with Monte Carlo simulations and experiments in superconductors.

The paper is organized as follows. In section 2 the covariant gaussian approximation in the symmetry broken phase is developed using the simplest toy model: the one dimensional spin chain equivalent mathematically to the double well anharmonic oscillator in quantum mechanics. The Dyson - Schwinger (DS) equations method is used and results for the two and four point correlators are compared with direct numerical calculations, Monte Carlo (MC) simulations as well as perturbation theory. In section 3 we apply CGA to the $O(2)$ invariant model and show how the corresponding Ward identities are derived. In section 4 the cluster Monte Carlo method appropriate for the calculation inside the symmetry broken phase is briefly described. The correlator of the order parameter of isotropic GL model in 3D is calculated with CGA. In section 5 we derive the expression for the magnetic penetration depth of an anisotropic superconductor and compare the CGA results with direct MC simulations and experimental data on penetration depth of several high T_c cuprates and discuss the results. Conclusions are given in section 6.

2. Hierarchy of variational conserving approximations defined as truncations of DS equations

2.1. A toy model and basic definitions

To present the approximation scheme we will make use of the simplest nontrivial model: statistical physics of a one dimensional classical chain that is equivalent to the quantum mechanics of the anharmonic oscillator. Our starting

point therefore will be the following free energy as a function of a single component order parameter (equivalently Euclidean (Matsubara) action of an anharmonic oscillator):

$$A = \frac{1}{\omega}\int dx\left\{\frac{1}{2}\left(\partial\phi\left(x\right)\right)^2 + \frac{a}{2}\phi\left(x\right)^2 + \frac{1}{4}\phi\left(x\right)^4 - J\left(x\right)\phi\left(x\right)\right\}. \tag{1}$$

The dimensionless coefficient ω, proportional to temperature T in statistical physics of classical chain or to $\hbar$ in quantum anharmonic oscillator, determines the strength of the (thermal or quantum) fluctuations. The normalization of the order parameter field $\phi\left(x\right)$ and the position x is such that ω is dimensionless (proportional to $\sqrt{Gi}$ where Gi is the Ginzburg number[4]) and the coefficient of interaction term is $1/4$. This free energy without external source ($J\left(x\right)=0$) has Z_2 symmetry, that is, invariant under $\phi\left(x\right)\rightarrow-\phi\left(x\right)$. The thermodynamics of this model is determined by the statistical sum

$$Z = \int \mathcal{D}\phi\left(x\right)e^{-A\left[\phi(x)\right]}. \tag{2}$$

The n-body correlator, the main object of interest in the present paper, is defined by

$$\left\langle\phi\left(x_1\right)\cdots\phi\left(x_n\right)\right\rangle = Z^{-1}\int_{\phi(x)}\phi\left(x_1\right)\cdots\phi\left(x_n\right)e^{-A\left[\phi(x)\right]}\Big|_{J=0}. \tag{3}$$

This full n-body correlator can be conveniently written[2] in terms of connected correlators denoted by $\left\langle\cdots\right\rangle_c$, while the later can be conveniently expressed via "cumulants" $\Gamma\left(x_1,\cdots,x_n\right)$. For example the simplest two body correlator can be written as

$$\left\langle\phi\left(x\right)\phi\left(y\right)\right\rangle = \left\langle\phi\left(x\right)\right\rangle\left\langle\phi\left(y\right)\right\rangle + \left\langle\phi\left(x\right)\phi\left(y\right)\right\rangle_c \equiv \varphi\left(x\right)\varphi\left(y\right) + G\left(x,y\right) = \varphi\left(x\right)\varphi\left(y\right) + \Gamma^{-1}\left(x,y\right) \tag{4}$$

Here the order parameter average is denoted by the "classical field" $\varphi\left(x\right)\equiv\left\langle\phi\left(x\right)\right\rangle$ and the two - body cumulant $\Gamma\left(x,y\right)$ is the inverse in the matrix sense to the connected correlator

$$\int_u \Gamma\left(x,u\right)G\left(u,y\right) = \delta\left(x-y\right). \tag{5}$$

Similarly the three - body connected correlator is expressed via cumulants as

$$\left\langle\phi\left(x\right)\phi\left(y\right)\phi\left(z\right)\right\rangle_c \equiv G_3\left(x,y,z\right) = -\int_{u,v,w} G\left(x,u\right)G\left(y,v\right)G\left(z,w\right)\Gamma\left(u,v,w\right). \tag{6}$$

From the functional integral in the presence of source $J\left(x\right)$, one can derive the equation of state (ES), the first of the infinite set of coupled DS equations for connected correlators :

$$J\left(x\right) = \left(-\partial^2 + a\right)\varphi\left(x\right) + \varphi\left(x\right)^3 + 3\varphi\left(x\right)G\left(x,x\right) + G_3\left(x,x,x\right). \tag{7}$$

To simplify the expression, we will set $\omega=1$ from now on. This always can be achieved by rescaling in 1D system since there are no ultraviolet (UV) or infrared (IR) divergences. The parameter ω will be reinstated when we need to use it to count the order of "loop expansion".

The second DS equation is the functional derivative of the equation of state,

$$\begin{aligned}\frac{\delta J\left(x\right)}{\delta\phi\left(y\right)} \equiv\ & \Gamma\left(x,y\right) = \left(-\partial_x^2 + a\right)\delta\left(x-y\right) + 3\delta\left(x-y\right)\varphi\left(x\right)^2 + 3\delta\left(x-y\right)G\left(x,x\right) \\ & +3\varphi\left(x\right)\int_u \Gamma\left(y,u\right)G_3\left(x,x,u\right) + \int_u \Gamma\left(y,u\right)G_4\left(x,x,x,u\right).\end{aligned} \tag{8}$$

The infinite set of equations is not useful unless a way to decouple higher order equations is proposed. The simplest one is the classical approximation.

2.2. Classical approximation and its variational interpretation

The classical approximation consists of neglecting the two and three body correlators in the equation of state, Eq.(7),

$$J(x) = \left(-\partial^2 + a\right)\varphi(x) + \varphi(x)^3\,, \tag{9}$$

so that the second and higher equations are decoupled from the first. Then the "minimization equation", that is just the on-shell ($J = 0$) ES,

$$\left(-\partial^2 + a\right)\varphi(x) + \varphi(x)^3 = 0, \tag{10}$$

is solved.

For $a < 0$ there are typically several solutions of this equation. Restricting ourselves to the translational invariant ones (namely excluding kinks), one has

$$\varphi(x) = 0, \pm v; \quad v = \sqrt{-a}. \tag{11}$$

Despite the fact that we know there is no spontaneous symmetry breaking in $d = 1$, a rather precise approximation scheme for a Z_2 invariant quantity emerges when one of the two "would be" symmetry broken solutions, say $\varphi(x) = +v$, is considered in the intermediate steps.

Note that despite the fact that the minimization principle involved only the one - body cumulant, $\varphi(x)$, one can still calculate the higher cumulants within the classical approximation. These are given by functional derivatives of the source $J(x)$ with respect to $\varphi(x)$ in truncated ES Eq.(9):

$$\Gamma_{cl}(x,y) = \frac{\delta J(x)}{\delta\varphi(y)} = (-\partial_x^2 + a + 3\varphi(x)^2)\delta(x-y)\,; \tag{12a}$$

$$\Gamma^3_{cl}(x,y,z) = \frac{\delta^2 J(x)}{\delta\varphi(y)\,\delta\varphi(z)} = 6\delta(x-y)\,\delta(x-z)\,\varphi(x)\,; \tag{12b}$$

$$\Gamma^4_{cl}(x,y,z,u) = \frac{\delta^3 J(x)}{\delta\varphi(y)\,\delta\varphi(z)\,\delta\varphi(u)} = 6\delta(x-y)\,\delta(x-z)\,\delta(x-u)\,. \tag{12c}$$

The cumulants beyond the fourth order vanish within this approximation.

The full correlator, a quantity invariant under the Z_2, in this approximation is:

$$P(x) \equiv \langle\phi(x)\,\phi(0)\rangle = v^2 + \Gamma^{-1}_{cl}(x,0)\,. \tag{13}$$

The matrix inversion of

$$\Gamma_{cl}(x,y) = \left(-\partial_x^2 + a + 3v^2\right)\delta(x-y) = \left(-\partial_x^2 + m^2\right)\delta(x-y) \tag{14}$$

as usual is performed in Fourier space, $\phi_k = \sum_k e^{-ikx}\phi(x)$. Here the mass is $m^2 = 2v^2$. Therefore the full correlator in momentum space is just

$$P(k) = \langle\phi_k\phi_{-k}\rangle = v^2\delta_k + \frac{1}{k^2+m^2}. \tag{15}$$

It can be corrected to "one loop" by calculating the "tadpole" diagram and takes the form

$$P(k) = v^2\delta_k + \omega\left\{2v\langle\phi_k\rangle + G_{cl}(k)\right\} = v^2\delta_k + \omega\left\{-\delta_k\sum\nolimits_p \frac{1}{p^2+m^2} + \frac{1}{k^2+m^2}\right\}, \tag{16}$$

where the fluctuation parameter ω has been reinstated. Returning to the configuration space, one has

$$P(x) = v^2 + \frac{\omega}{2\pi}\int_{k=-\infty}^{\infty}\frac{e^{ikx}-1}{k^2+m^2} = v^2 + \frac{\omega}{2m}\left(e^{-m|x|}-1\right). \tag{17}$$

This is compared in Figure 1 (shown as dashed blue lines) with the numerically calculated correlator (see Appendix A) and cluster Monte Carlo simulations (see details in section 4.2) for negative a and $\omega = 1$. One notices that the classical approximation exhibits long range order at negative a, which is definitely wrong in the case of one dimension as clearly shown by both numerical calculation and MC simulations. The classical approximation that was obtained

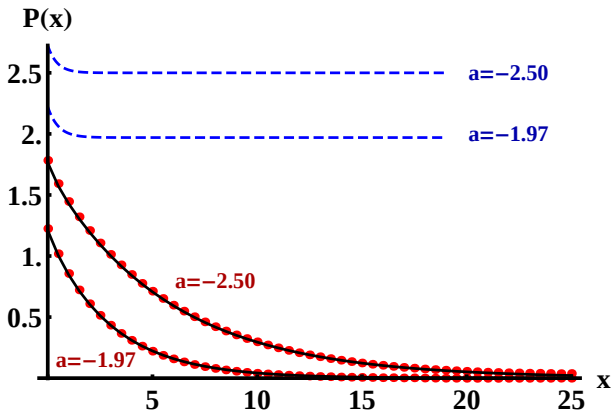

Figure 1: Correlator in real space $P(x)$ calculated by different methods. The parameter ω is taken to be 1 (can be scaled away) and values of $a = -1.97, -2.5$ are given. Black lines are direct spectrum calculations (see Appendix A). Red dots are Monte Carlo simulations with error bars smaller than the size of dots. Dashed blue lines are the classical approximation, Eq.(17).

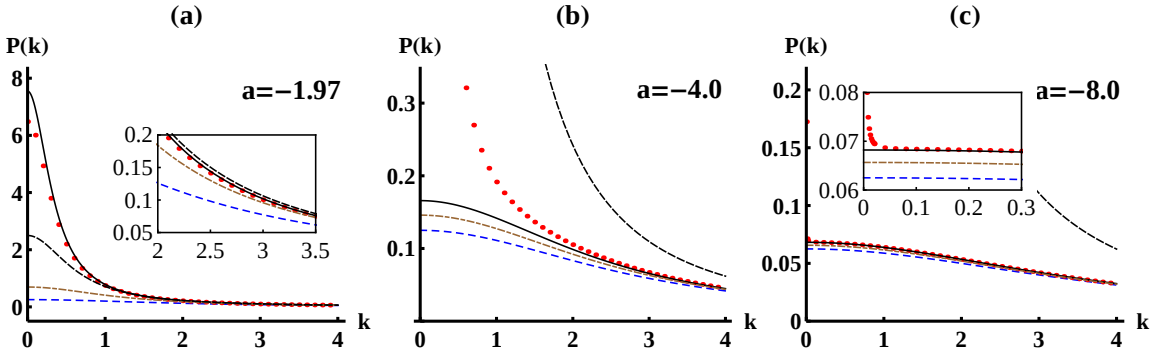

Figure 2: Correlator in momentum space calculated by different methods at $a = -1.97, -4, -8$. Red dots are direct spectrum calculations (see Appendix A). Dashed blue line is the classical approximation, Eq.(15). The black line is CGA around broken phase solution of the minimization equations, Eq.(54). Dashed black is gaussian approximation in the symmetric phase, Eq.(31). Brown dashed dot line is the naive gaussian approximation in the "would be" broken phase, Eq.(36). The erroneous delta function part at zero momentum is not shown in this figure. Insets in (a) and (c) show amplifications of the corresponding small regions.

by an ad hoc truncation of the exact ES can be made a part of a systematically improvable scheme by considering the arbitrarily omitted last two terms in Eq.(7) as a perturbation.

The minimization equation Eq.(10) can be interpreted variationally as minimizing the quantum mechanical double well Hamiltonian

$$H = -\frac{1}{2}\frac{\partial^2}{\partial\phi^2} + \frac{a}{2}\phi^2 + \frac{1}{4}\phi^4, \tag{18}$$

on the set of coherent states wave functions (become functionals in higher dimensional models):

$$\psi(\phi) = \left(\frac{1}{2\pi g}\right)^{1/4} \exp\left[-\frac{1}{4g}(\phi - \varphi)^2\right]. \tag{19}$$

The parameter g, square of the width of the gaussian wave function, is arbitrary but fixed. The expectation value of energy

$$E(\varphi, g) = \langle\psi(\phi)|H|\psi(\phi)\rangle = \frac{1}{8g} + \frac{a}{2}g + \frac{3}{4}g^2 + \frac{1}{2}(a + 3g)\varphi^2 + \frac{1}{4}\varphi^4 \tag{20}$$

is minimized with respect to the shift φ. This leads to the translational invariant form of the classical equation Eq.(10) for small g (localized gaussian).

In principle one can do better. Variationally one can optimize not just the shift of the gaussian wave function, but also the width g.

2.3. Gaussian variational principle

Optimization of the energy Eq.(20) with respect to both parameters φ and g would give us the minimization equations of the following form[15]

$$\frac{\delta}{\delta\varphi}E(\varphi,g)=(a+3g)\varphi+\varphi^3=0; \tag{21}$$

$$\frac{\delta}{\delta g}E(\varphi,g)=-\frac{1}{8g^2}+\frac{a}{2}+\frac{3}{2}g+\frac{3}{2}\varphi^2=0. \tag{22}$$

We will see these two equations coincide with the "two - body" truncation of the DS equations for $J(x)=0$ under the assumption of translational invariance.

Instead of truncating out the two-body and higher cumulant, like in the classical approximation, one can truncate the DS set of equations starting from the three-body cumulant. Of course the approximation becomes more complicated. Indeed let us truncate the two lowest order DS equations, Eq.(7) and Eq.(8), leaving out only the last term in ES, Eq.(7)

$$J(x)=\left(-\partial^2+a\right)\varphi(x)+\varphi(x)^3+3\varphi(x)G^{tr}(x,x), \tag{23}$$

and the last two terms of the second DS equation, Eq.(8),

$$\Gamma^{tr}(x,y)=\left(-\partial_x^2+a\right)\delta(x-y)+3\delta(x-y)\varphi(x)^2+3\delta(x-y)G^{tr}(x,x). \tag{24}$$

Here the superscript "tr" indicates that the correlators satisfy the approximated truncated equations instead of the exact ones.

In the naive gaussian variational principle approach[15], one considers these equations as minimization equations with $\varphi(x)$ and $G^{tr}(x,y)$ identified as the connected correlator inverse to $\Gamma^{tr}(x,y)$ in the matrix sense. Let us assume the space translational invariance leading to

$$\varphi(x)=\varphi,\ G^{tr}(x,y)=g^{tr}(x-y)=\sum\nolimits_k e^{ik(x-y)}g_k^{tr}, \tag{25}$$

so that the minimization equations for $J=0$ take the form

$$0=a\varphi+\varphi^3+3\varphi\sum\nolimits_k g_k^{tr}, \tag{26}$$

and

$$\frac{1}{g_k^{tr}}=k^2+a+3\varphi^2+3\sum\nolimits_k g_k^{tr}. \tag{27}$$

One already recognizes in Eq.(26) the shift equation Eq.(21) while identifying the width of the gaussian wave function with the correlator on site $g=g^{tr}(x-x)=\sum_k g_k^{tr}$. The second equation commonly called the gap equation can be rearranged as:

$$g_k^{tr}=\frac{1}{k^2+a+3\varphi^2+3g}. \tag{28}$$

By summing over all momenta k one obtains

$$g=\sum\nolimits_k\frac{1}{k^2+a+3\varphi^2+3g}=\frac{1}{2\sqrt{a+3\varphi^2+3g}}. \tag{29}$$

Taking the square of this equation one arrives at Eq.(22).

One can see from Eq.(21) that the symmetric solution $\varphi=0$ exists for any a and is given by a root of the cubic equation

$$g_s^3+\frac{a}{3}g_s^2-\frac{1}{12}=0, \tag{30}$$

where the subscript "s" stands for "symmetric". Accordingly the connected correlator is

$$g_k^{tr} = \frac{1}{k^2 + m_s^2} \tag{31}$$

with a mass of

$$m_s^2 = a + 3g_s. \tag{32}$$

In the symmetric phase it coincides with the full 2-body correlator and is given in Figure 2 as a black dashed line.

The would be broken solution can be written as

$$\varphi^2 = -a - 3g_a, \tag{33}$$

with g_a satisfying another cubic equation

$$g_a^3 + \frac{a}{3} g_a^2 + \frac{1}{24} = 0. \tag{34}$$

Here the subscript "a" stands for "asymmetric". The solution exists only in the double well for $a < -(3/2)^{5/3} \approx -1.966$. The correlator in this case has a mass

$$m_a^2 = -2a - 6g_a = 2\varphi^2. \tag{35}$$

The order parameter correlator takes the form

$$P^{tr}(k) = \varphi^2 \delta_k + \frac{1}{k^2 + m_a^2}. \tag{36}$$

This is shown as a brown dashed dot line in Figure 2. One observes that while the symmetric solution known to be precise at positive a, it becomes much worse at negative a with large absolute value than the one obtained with apparently erroneous symmetry broken solution.

2.4. The covariant gaussian approximation

In the classical approximation truncation of the DS equation means that the off shell (nonzero $J(x)$) equation of state is modified. The higher cumulants are obtained by differentiation of the source with respect to the shift $\varphi(x)$. One can try the same strategy within the gaussian approximation. In the next section, while considering a more complicated $O(2)$ invariant model, we will focus on an advantage of this approach: it preserves the Ward identities of linearly represented symmetries of the system. Now we concentrate on technicalities of the calculation.

For convenience we reprint here the first and second truncated DS equations,

$$J(x) = \left(-\partial^2 + a\right)\varphi(x) + \varphi(x)^3 + 3\varphi(x) G^{tr}(x,x), \tag{37}$$

and

$$\Gamma^{tr}(x,y) = \left(-\partial_x^2 + a\right)\delta(x-y) + 3\delta(x-y)\varphi(x)^2 + 3\delta(x-y) G^{tr}(x,x). \tag{38}$$

The truncated correlator $G^{tr}(x,y)$ should be considered as a functional of $\varphi(x)$ that is determined by the above two equations with the condition

$$\int_y \Gamma^{tr}(x,y) G^{tr}(y,z) = \delta(x-z). \tag{39}$$

As in the case of classical approximation, the "true" correlator is derived by taking derivative of the shift equation Eq.(37),

$$\Gamma(x,y) \equiv \frac{\delta}{\delta\varphi(y)} J(x) = \left\{-\partial^2 + a + 3\varphi(x)^2 + 3G^{tr}(x,x)\right\}\delta(x-y) + 3\varphi(x)\frac{\delta}{\delta\varphi(y)} G^{tr}(x,x). \tag{40}$$

In contrast Γ^{tr} should be viewed as a variational parameter only. The first term is just $\Gamma^{tr}(x,y)$, while the second term is the "chain correction"[17]. The origin of the notation comes from the perturbative analysis of the contributions. Denote it by

$$\frac{\delta}{\delta\varphi(z)} G^{tr}(x,y) \equiv C(z|x,y), \tag{41}$$

and it can be calculated by differentiation of the identity Eq.(39)

$$\int_u \frac{\delta}{\delta\varphi(z)}\Gamma^{tr}(x,u)\,G^{tr}(u,y) + \int_u \Gamma^{tr}(x,u)\,\frac{\delta}{\delta\varphi(z)}G^{tr}(u,y) = 0. \tag{42}$$

Multiplying from the left by the matrix G^{tr},one obtains

$$C(z|x,y) = -\int_{u,v} G^{tr}(x,v)\frac{\delta\Gamma^{tr}(v,u)}{\delta\varphi(z)}G^{tr}(u,y). \tag{43}$$

Taking derivative of the gap equation, Eq.(38), results in

$$\frac{\delta\Gamma^{tr}(v,u)}{\delta\varphi(z)} = 6\varphi(u)\,\delta(z-v)\delta(v-u) + 3\delta(v-u)C(z|v,v). \tag{44}$$

Thus the chain equation becomes

$$C(z|x,y) = -6\varphi(z)\,G^{tr}(x,z)G^{tr}(z,y) - 3\int_v G^{tr}(x,v)G^{tr}(v,y)C(z|v,v). \tag{45}$$

Note that this equation is linear in the chain function C and can be conveniently solved by iteration. The problem is that the number of unknowns is very large. However there are two observations that greatly reduce the complexity. First the argument z is the same on both the right and left hand side and therefore is just a parameter. The second is that the right hand side of the equation depends only on $C(z|v,v)$ with two last arguments identical. Consequently one can first solve the particular case of $y = x$:

$$C(z|x,x) = -6\varphi(z)\,G^{tr}(x,z)G^{tr}(z,x) - 3\int_v G^{tr}(x,v)G^{tr}(v,x)C(z|v,v). \tag{46}$$

This particular chain is in fact the only quantity we need in order to calculate the "covariant" correction to the correlator in Eq.(40):

$$\Delta\Gamma(x,y) \equiv \Gamma(x,y) - \Gamma^{tr}(x,y) = 3\varphi(x)\,C(y|x,x)\,. \tag{47}$$

We will not need temporarily the chain function for arbitrary arguments.

Using the translation invariance, one sees the function depends on just one variable:

$$C(z|x,x) = c(z-x)\,. \tag{48}$$

It obeys

$$c(z-x) = -6g^{tr}(x-z)g^{tr}(z-x)\varphi - 3\int_v g^{tr}(x-v)g^{tr}(v-x)c(z-v). \tag{49}$$

In momentum space the linear equation becomes algebraic for one variable only,

$$c_k = -6\varphi\sum\nolimits_p g^{tr}_p g^{tr}_{k-p} - 3\sum\nolimits_p g^{tr}_p g^{tr}_{k-p}c_k, \tag{50}$$

which can be easily solved as

$$c_k = -\frac{6\varphi f_k}{1+3f_k}. \tag{51}$$

Here the "fish" diagram is

$$f_k \equiv \sum\nolimits_p g^{tr}_p g^{tr}_{k-p} = \frac{1}{m_a}\frac{1}{k^2+4m_a^2}. \tag{52}$$

Substituting this into the expression for the cumulant correction in the momentum space, one gets

$$\Delta\Gamma_k = 3\varphi c_k = -\frac{18\varphi^2}{f_k^{-1}+3}. \tag{53}$$

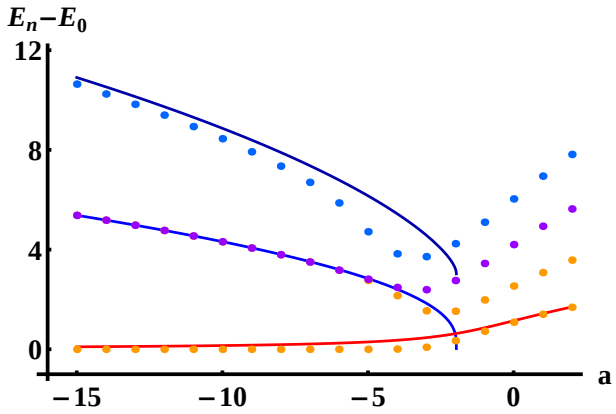

Figure 3: Poles and excitations. Dots are excitations $E_n - E_0$ calculated by exact numerical diagonalization of the double well potential. The red line is the mass of the two point correlator in symmetric phase Eq.(32). The blue and dark blue lines are poles in the "broken" phase Eq.(55) calculated by CGA.

The order parameter correlator in CGA finally is

$$P(k) = \varphi^2 \delta_k + \left(k^2 + m_a^2 - \frac{18\varphi^2}{f_k^{-1} + 3} \right)^{-1} = \frac{m_a^2}{2} \delta_k + \frac{k^2 + 4m_a^2 + \frac{3}{m_a}}{\left(k^2 + M_1^2\right)\left(k^2 + M_2^2\right)}, \tag{54}$$

where

$$M_{1,2}^2 = \frac{1}{2m_a} \left(3 + 5m_a^3 \pm 3\sqrt{1 + 6m_a^3 + m_a^6} \right). \tag{55}$$

As an exact statement and reliable simulations, Figure 1, shows there is no symmetry breaking in this model and thus the appearance of the delta function is as erroneous as in the classical approximation. Eq.(54) at $k \neq 0$ is presented as a black line in Figure 2, together with results calculated by different methods in the momentum space.

Eq.(54) also demonstrates that there are poles and they do approximate well with excitations corresponding to the double well bound states, as one can see in Figure 3. In Figure 4 we show results of a more complicated invariant correlator $P_2(k) \equiv \int_x e^{-ikx} \left\langle \phi(x)^2 \phi(0)^2 \right\rangle$ calculated within CGA as well as results of exact numerical diagonalization. Details of the calculations can be found in Appendix B.

2.5. Variational interpretation of CGA

Generally cumulants are collected in the so called effective action[2], so that

$$A_{eff}[\varphi] = \sum_n \Gamma^n(x_1, \cdots, x_n) \varphi(x_1) \cdots \varphi(x_n). \tag{56}$$

The question arises whether the CGA cumulants defined in the previous subsection can be obtained in the way from an approximated effective action. The answer is yes. Although due to its complexity the action is of little use in actual computation and the DS equations truncation method is far superior. However it will be useful conceptually in the next section to discuss the symmetry properties of the approximation that are of crucial importance in applications.

As we have seen already the minimization equations shared by the naive gaussian approximation and CGA are equivalent to minimization of the expectation value of Hamiltonian, Eq.(18), on a set of general gaussian wave functions, Eq.(19). The CGA correlators can be obtained from a truncation of the (in principle exact) Cornwall-Jackiw-Tomboulis (CJT) functional[18] that is a double Legendre transformation. The action contains infinite number of terms:

$$A_{eff}[\varphi(x), G] = A[\varphi(x)] + \frac{1}{2}\mathrm{Tr}\left[\log G^{-1}\right] + \frac{1}{2}\mathrm{Tr}\left[D^{-1}G - 1\right] + \frac{3}{2}\int_x \varphi(x)^2 G(x,x) + \frac{3}{4}\int_x G(x,x)^2 + \cdots. \tag{57}$$

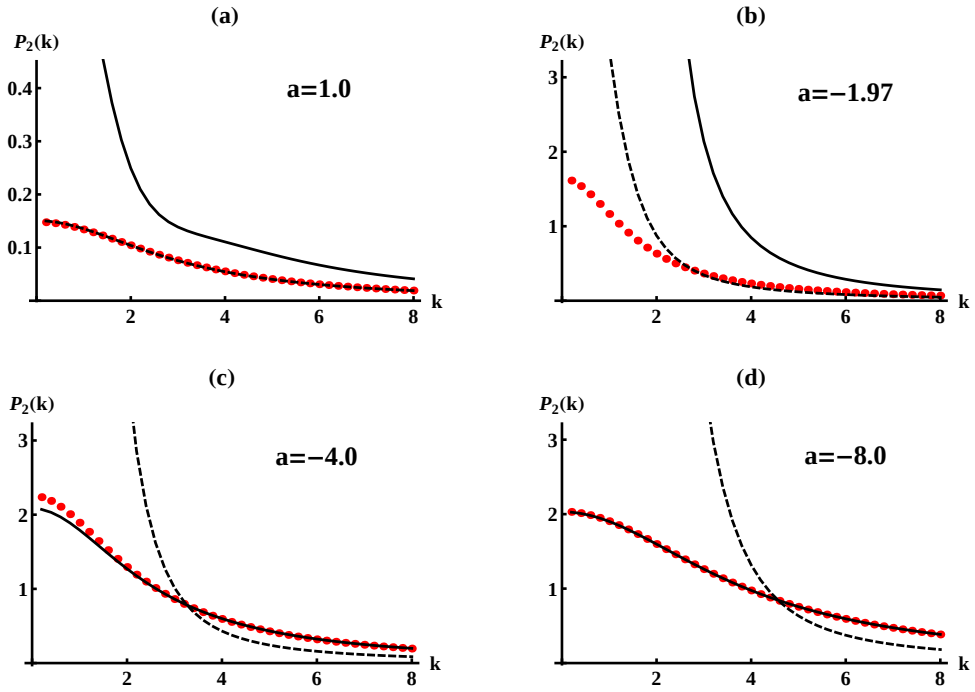

Figure 4: Correlator of composite operator $\phi^2(r)$ at $a = 1, -1.97, -4, -8$. The red dots are exact numerically calculated results. Black lines are CGA results starting from the broken solution of minimization equations. Black dashed lines are results starting from the symmetric solution.

Here

$$D^{-1}(x,y) = \left(-\partial_x^2 + a\right)\delta(x-y), \tag{58}$$

and each matrix element of the correlator, $G(x,y)$, should be understood as a functional of the order parameter $\varphi(x)$ determined by the minimization equation $\delta A/\delta G = 0$. Traces and logarithm are also understood in the matrix sense.

Let us truncate this infinite series to the terms explicitly written in Eq.(57). The minimization condition becomes just the gap equation, Eq.(24), for the truncated correlator that can be written in the following form:

$$-\frac{1}{2}\left(G^{tr}\right)^{-1}(x,y) + \frac{1}{2}D^{-1}(x,y) + \frac{3}{2}\varphi(x)^2\,\delta(x-y) + \frac{3}{2}G^{tr}(x,x)\,\delta(x-y), \tag{59}$$

and vanish if the gap equation is obeyed. The first functional derivative of A_{eff} with respect to $\varphi(x)$ reproduces $J(x)$ of the truncated shift equation,

$$J(x) = \frac{\delta A_{eff}}{\delta\varphi(x)} = \left(-\partial_x^2 + a\right)\varphi(x) + \varphi(x)^3 + 3\varphi(x)\,G^{tr}(x,x), \tag{60}$$

that coincides with Eq.(23). This means that the second derivative of the effective action coincides with the CGA correlator rather than with the gaussian truncated correlator.

3. Why all the Ward identities are obeyed by the CGA correlators

3.1. Importance of symmetry preservation in the phase with broken symmetry

In this section we focus on the preservation of all the symmetry properties of correlators within CGA. These properties are crucially important for making an approximation useful. The issue is obviously crucial when the symmetry is spontaneously broken since the low energy properties are determined by the Goldstone bosons[1] (GB), massless modes whose very existence hinges on the symmetry breaking. Consequences of the symmetry whether

broken or not in terms of correlators are expressed by the Ward identities[2]. While the classical approximation obeys the Ward identities, the naive gaussian approximation unfortunately does not.

We demonstrate here that the CGA corrections to the naive gaussian correlators are just enough to make the full correlators consistent with the Ward identities. This allows one in particular to take into account accurately the Goldstone bosons. In addition the "charge conserving"[16] property of the approximation is imperative if one discusses renormalizability (small distance cutoff dependence) with respect to ultraviolet divergencies. In $d \geq 2$ the reason that the UV cutoff dependence may be absorbed by the the renormalized wave function and coupling constants hinges on the symmetry considerations[2].

To this end it will be more instructive to consider a continuous symmetry rather than the discrete symmetry Z_2, since we would like to involve the GB. The model possessing the simplest continuous symmetry, $O(2)$, has the following free energy:

$$A = \frac{1}{2\omega}\int_{\mathbf{r}}\left\{\left(\nabla\phi^a(\mathbf{r})\right)^2 + a\phi^a(\mathbf{r})\,\phi^a(\mathbf{r}) + \frac{1}{2}\left(\phi^a(\mathbf{r})\,\phi^a(\mathbf{r})\right)^2\right\}, \tag{61}$$

where $a = 1, 2$. We use two real fields, although very often a complex field is employed. The dimensionality d will be kept arbitrary for the time being. The $O(2)$ invariance is expressed in a functional form as independence of the effective action under the transformation,

$$A_{eff}\left[R^{ab}(\theta)\,\varphi^b(\mathbf{r})\right] = A_{eff}\left[\varphi^a(\mathbf{r})\right], \tag{62}$$

for any angle θ. Here $R^{ab}(\theta)$ is the global symmetry rotation matrix. The infinitesimal transformation, using the chain rule relates this to the ES:

$$0 = A_{eff}\left[\varphi^a(\mathbf{r}) + \theta\varepsilon^{ab}\varphi^b(\mathbf{r})\right] - A_{eff}\left[\varphi^a(\mathbf{r})\right] \Longrightarrow \int_{\mathbf{r}}\frac{\delta A_{eff}}{\delta\varphi^a(\mathbf{r})}\varepsilon^{ab}\varphi^b(\mathbf{r}) = \int_{\mathbf{r}} J^a(\mathbf{r})\,\varepsilon^{ab}\varphi^b(\mathbf{r}) = 0. \tag{63}$$

Functional derivatives of this equation with respect to $\varphi^a(\mathbf{r})$ generate all the Ward identities expressing the symmetry. The first two are

$$0 = \frac{\delta}{\delta\varphi^a(\mathbf{r})}\int_{\mathbf{r}'} J^e(\mathbf{r}')\,\varepsilon^{ef}\varphi^f(\mathbf{r}')\Big|_{J=0} = \int_{\mathbf{r}'}\Gamma^{ae}(\mathbf{r},\mathbf{r}')\,\varepsilon^{ef}\varphi^f(\mathbf{r}'); \tag{64a}$$

$$\begin{aligned} 0 &= \frac{\delta^2}{\delta\varphi^b(\mathbf{r}_2)\,\delta\varphi^a(\mathbf{r}_1)}\int_{\mathbf{r}'} J^e(\mathbf{r}')\,\varepsilon^{ef}\varphi^f(\mathbf{r}')\Big|_{J=0} \\ &= \int_{\mathbf{r}'}\Gamma^{abe}(\mathbf{r}_1,\mathbf{r}_2,\mathbf{r}')\,\varepsilon^{ef}\varphi^f(\mathbf{r}') + \Gamma^{ae}(\mathbf{r}_1,\mathbf{r}_2)\,\varepsilon^{eb} + \Gamma^{eb}(\mathbf{r}_1,\mathbf{r}_2)\,\varepsilon^{ea}. \end{aligned} \tag{64b}$$

The first equation on shell gives the Goldstone theorem. Indeed taking $\varphi^1 = \varphi$, $\varphi^2 = 0$ in momentum space it reads

$$\Gamma^{a2}(\mathbf{k} = \mathbf{0}) = 0. \tag{65}$$

3.2. Proof of the conserving property of CGA

Here we use two quite different arguments to demonstrate that CGA obeys the Ward identities. The first is to prove Eq.(63) directly within a specific model using the CGA (truncated) off shell ES and the gap equation. In the $O(2)$ model, the ES is,

$$J^a(\mathbf{r}) = \left(-\nabla^2 + a\right)\varphi^a(\mathbf{r}) + \varphi^a(\mathbf{r})\,\varphi^e(\mathbf{r})\,\varphi^e(\mathbf{r}) + \omega\varphi^a(\mathbf{r})\,G^{ee}_{tr}(\mathbf{r},\mathbf{r}) + 2\omega\varphi^e(\mathbf{r})\,G^{ae}_{tr}(\mathbf{r},\mathbf{r}), \tag{66}$$

and the gap equation takes the form

$$\Gamma^{ab}_{tr}(\mathbf{r}_1,\mathbf{r}_2) = \left\{\delta^{ab}\left(-\nabla^2_{r_1} + a + \varphi^e(\mathbf{r}_1)\,\varphi^e(\mathbf{r}_1) + \omega G^{ee}_{tr}(\mathbf{r}_1,\mathbf{r}_1)\right) + 2\varphi^a(\mathbf{r})\,\varphi^b(\mathbf{r}) + 2\omega G^{ab}_{tr}(\mathbf{r}_1,\mathbf{r}_1)\right\}\delta(\mathbf{r}_1 - \mathbf{r}_2). \tag{67}$$

Substituting Eq.(66) into the functional Ward identity, Eq.(63), one obtains:

$$\int_{\mathbf{r}}\left\{-\nabla^2\varphi^a(\mathbf{r}) + \left(a + \varphi^e(\mathbf{r})\,\varphi^e(\mathbf{r}) + \omega G^{ee}_{tr}(\mathbf{r},\mathbf{r})\right)\varphi^a(\mathbf{r}) + 2\omega G^{ae}_{tr}(\mathbf{r},\mathbf{r})\,\varphi^e(\mathbf{r})\right\}\varepsilon^{ab}\varphi^b(\mathbf{r}). \tag{68}$$

The second term in the curly brackets vanishes identically, while the first vanishes after integration by parts,

$$\int_{\mathbf{r}} \varepsilon^{ab}\varphi^b(\mathbf{r})\nabla^2\varphi^a(\mathbf{r}) = -\int_{\mathbf{r}} \varepsilon^{ab}\nabla\varphi^b(\mathbf{r})\nabla\varphi^a(\mathbf{r}) = 0. \tag{69}$$

The only nontrivial term therefore is the last one,

$$\int_{\mathbf{r}} \varphi^b(\mathbf{r})\varepsilon^{ba}G^{ae}_{tr}(\mathbf{r},\mathbf{r})\varphi^e(\mathbf{r}). \tag{70}$$

To show that this term also vanishes, let us multiply the gap equation Eq.(67) by $G^{bc}_{tr}(\mathbf{r}_2,\mathbf{r})$ and integrate over $\mathbf{r}_2$:

$$\left(-\nabla^2_{\mathbf{r}_1} + a + (\varphi^e(\mathbf{r}_1))^2 + \omega G^{ee}_{tr}(\mathbf{r}_1,\mathbf{r}_1)\right)G^{ac}_{tr}(\mathbf{r}_1,\mathbf{r}) + 2\omega\left(\varphi^a(\mathbf{r}_1)\varphi^b(\mathbf{r}_1) + G^{ab}_{tr}(\mathbf{r}_1,\mathbf{r}_1)\right)G^{bc}_{tr}(\mathbf{r}_1,\mathbf{r}) = \delta^{ac}\delta(\mathbf{r}_1-\mathbf{r}). \tag{71}$$

Multiply this by ε^{ac}, summing over a,c and taking $\mathbf{r}=\mathbf{r}_1$ at the end. Thus, the scalar equation simplifies due to symmetry $G^{ac}_{tr}(\mathbf{r},\mathbf{r}) = G^{ca}_{tr}(\mathbf{r},\mathbf{r})$ into

$$-\varepsilon^{ac}\nabla^2_{\mathbf{r}'}G^{ac}_{tr}(\mathbf{r}',\mathbf{r}_1)|_{\mathbf{r}'=\mathbf{r}_1} + 2\varepsilon^{ac}\varphi^a(\mathbf{r}_1)\varphi^b(\mathbf{r}_1)G^{bc}_{tr}(\mathbf{r}_1,\mathbf{r}_1) + 2\omega\varepsilon^{ac}G^{ab}_{tr}(\mathbf{r}_1,\mathbf{r}_1)G^{bc}_{tr}(\mathbf{r}_1,\mathbf{r}_1) = 0. \tag{72}$$

The last term vanishes since $G^{ab}_{tr}(\mathbf{r},\mathbf{r})G^{bc}_{tr}(\mathbf{r},\mathbf{r})$ is symmetric under $a\leftrightarrow c$. Finally integrating over $\mathbf{r}_1$, the first term vanishes as a full derivative and we arrive at Eq.(70).

The second method to demonstrate the Ward identities utilizes the known effective potential within the CGA, given in the previous section, Eq.(57). A general observation is that it is written covariantly as an $O(2)$ scalar and in addition the CGA off shell minimization equations are covariant, namely J^a and φ^a are $O(2)$ vectors, while G^{ab}_{tr} is a tensor. This was what originally motivated the term "CGA"[17]. Indeed, if $\varphi^a(\mathbf{r})$ and $G^{ab}_{tr}(\mathbf{r})$ are solutions of the minimization equations Eq.(66) and Eq.(67), so are $R^{ae}(\theta)\varphi^e(\mathbf{r})$ and $R^{ae}(\theta)R^{bf}(\theta)G^{ef}_{tr}(\mathbf{r})$, provided the source $J(\mathbf{r})$ was rotated as well. This means that the CGA effective action is invariant just as the exact one in Eq.(62) and all the Ward identities follow. The truncation of the higher correlators doesn't violate the covariance of φ^a and G^{ab}_{tr}, and therefore definition of correlator via derivatives of J keeps all the Ward identities.

The covariance proof of CGA can be extended to any symmetry linearly represented in the free energy and to statistical physics and (relativistic or not) many - body system involving fermionic, gauge field as long as the representation of the symmetry is linear or the truncation is covariant.

3.3. How it all works in $d = 3$

The proof of Ward identities is rather formal. As an example, let us see explicitly the $O(2)$ invariant model in dimension $d = 3$. The shift and gap equations in momentum space for the asymmetric order parameter along the direction 1, $\varphi^1 = \varphi$, $\varphi^2 = 0$, are

$$0 = a\varphi + \varphi^3 + \omega\varphi\sum_{\mathbf{k}}\left(G^{22}_{tr}(\mathbf{k}) + 3G^{11}_{tr}(\mathbf{k})\right); \tag{73a}$$

$$\Gamma^{ab}_{tr}(\mathbf{k}) = \delta^{ab}\left(k^2 + a + \varphi^2\right) + 2\varphi^a\varphi^b + \omega\sum_{\mathbf{k}}\left(\delta^{ab}G^{cc}_{tr}(\mathbf{k}) + 2G^{ab}_{tr}(\mathbf{k})\right). \tag{73b}$$

Due to remaining Z_2 symmetry $\phi^2\to-\phi^2$, the "mixed" correlator G^{12}_{tr} vanishes and the diagonal components of the cumulant take the form,

$$\Gamma^{11}_{tr} = k^2 + m_1^2;\ \ \Gamma^{22}_{tr} = k^2 + m_2^2. \tag{74}$$

This leads to the following set of algebraic equations for the two masses and φ:

$$0 = a + \varphi^2 + \frac{3\omega}{2\pi^2}\left(\Lambda - \frac{\pi m_1}{2}\right) + \frac{\omega}{2\pi^2}\left(\Lambda - \frac{\pi m_2}{2}\right); \tag{75a}$$

$$m_1^2 = a + 3\varphi^2 + \frac{3\omega}{2\pi^2}\left(\Lambda - \frac{\pi m_1}{2}\right) + \frac{\omega}{2\pi^2}\left(\Lambda - \frac{\pi m_2}{2}\right); \tag{75b}$$

$$m_2^2 = a + \varphi^2 + \frac{\omega}{2\pi^2}\left(\Lambda - \frac{\pi m_1}{2}\right) + \frac{3\omega}{2\pi^2}\left(\Lambda - \frac{\pi m_2}{2}\right). \tag{75c}$$

The UV cutoff Λ can be absorbed into the renormalized coupling

$$a_r = a + \frac{2\omega}{\pi^2}\Lambda. \tag{76}$$

The solution that exists only for $a_r < 0.03935\omega^2$ is given in Appendix C (a symmetric solution, $\varphi = 0$, that exists for all values of $a_r > 0$ is also given there).

The conclusion is that G^{ab}_{tr} is massive, namely does not have zero modes. However, as explained in the previous section, the naive gaussian correlator G^{ab}_{tr} is not the CGA correlator. The later is given by the derivative of Eq.(66),

$$\Gamma^{ab}(\mathbf{x},\mathbf{y}) = \Gamma^{ab}_{tr}(\mathbf{x},\mathbf{y}) + \omega\left[\varphi^a(\mathbf{x})\frac{\delta}{\delta\varphi^b(\mathbf{y})}G^{ee}_{tr}(\mathbf{x},\mathbf{x}) + 2\varphi^e(\mathbf{x})\frac{\delta}{\delta\varphi^b(\mathbf{y})}G^{ae}_{tr}(\mathbf{x},\mathbf{x})\right]. \tag{77}$$

The first term on the right hand side of the above equation is just the inverse to G^{ab}_{tr}, while the second term gives the correction $\Delta\Gamma^{ab}(\mathbf{x},\mathbf{y})$ containing the following chain function

$$\frac{\delta}{\delta\varphi^c(\mathbf{z})}G^{ab}_{tr}(\mathbf{x},\mathbf{y}) \equiv C^{c|ab}(\mathbf{z}|\mathbf{x},\mathbf{y}). \tag{78}$$

It is calculated from the chain equation in momentum space for the relevant quantity $c^{c|ab}_{\mathbf{k}}$ with the same Fourier transform defined as in section 2,

$$\begin{aligned} & c^{a|bc}_{\mathbf{k}} + \omega\left(3\delta_{b1}\delta_{c1}f^{11}_{\mathbf{k}} + \delta_{b2}\delta_{c2}f^{22}_{\mathbf{k}}\right)c^{a|11}_{\mathbf{k}} + 2\omega\left(\delta_{b2}\delta_{c1} + \delta_{b1}\delta_{c2}\right)f^{12}_{\mathbf{k}}c^{a|12}_{\mathbf{k}} + \omega\left(\delta_{b1}\delta_{c1}f^{11}_{\mathbf{k}} + 3\delta_{b2}\delta_{c2}f^{22}_{\mathbf{k}}\right)c^{a|22}_{\mathbf{k}} \\ = \; & -2\varphi\left[3\delta_{a1}\delta_{b1}\delta_{c1}f^{11}_{\mathbf{k}} + \delta_{a2}\left(\delta_{b1}\delta_{c2} + \delta_{b2}\delta_{c1}\right)f^{12}_{\mathbf{k}} + \delta_{a1}\delta_{b2}\delta_{c2}f^{22}_{\mathbf{k}}\right]. \end{aligned} \tag{79}$$

Here the explicit expression for the "fish" integral,

$$f^{ab}_{\mathbf{k}} = \sum\nolimits_{\mathbf{p}} g^a_{tr}(\mathbf{p})\, g^b_{tr}(\mathbf{k}-\mathbf{p}), \tag{80}$$

is listed in Appendix C. The only nonzero components of $c^{c|ab}_{\mathbf{k}}$ are:

$$c^{1|11}_{\mathbf{k}} = -\frac{2\varphi f^{11}_{\mathbf{k}}(3 + 8\omega f^{22}_{\mathbf{k}})}{1 + 3\omega\left(f^{11}_{\mathbf{k}} + f^{22}_{\mathbf{k}}\right) + 8\omega^2 f^{11}_{\mathbf{k}} f^{22}_{\mathbf{k}}}; \tag{81a}$$

$$c^{1|22}_{\mathbf{k}} = -\frac{2\varphi f^{22}_{\mathbf{k}}}{1 + 3\omega\left(f^{11}_{\mathbf{k}} + f^{22}_{\mathbf{k}}\right) + 8\omega^2 f^{11}_{\mathbf{k}} f^{22}_{\mathbf{k}}}; \tag{81b}$$

$$c^{2|12}_{\mathbf{k}} = c^{2|21}_{\mathbf{k}} = -\frac{2\varphi f^{12}_{\mathbf{k}}}{1 + 2\omega f^{12}_{\mathbf{k}}}. \tag{81c}$$

Substituting this into the expression of the cumulant correction in the momentum space

$$\Delta\Gamma^{11}_{\mathbf{k}} = \omega\varphi\left(3c^{1|11}_{\mathbf{k}} + c^{1|22}_{\mathbf{k}}\right); \qquad \Delta\Gamma^{22}_{\mathbf{k}} = 2\omega\varphi c^{2|21}_{\mathbf{k}}, \tag{82}$$

one gets for zero momentum the mass of Goldstone mode:

$$m^2_{GB} = m^2_2 + \Delta\Gamma^{22}_{\mathbf{k}=0} = 0. \tag{83}$$

Therefore the GB reappears in CGA. Similarly more complicated correlators can be calculated and other Ward identities like Eq.(64b) can be explicitly checked.

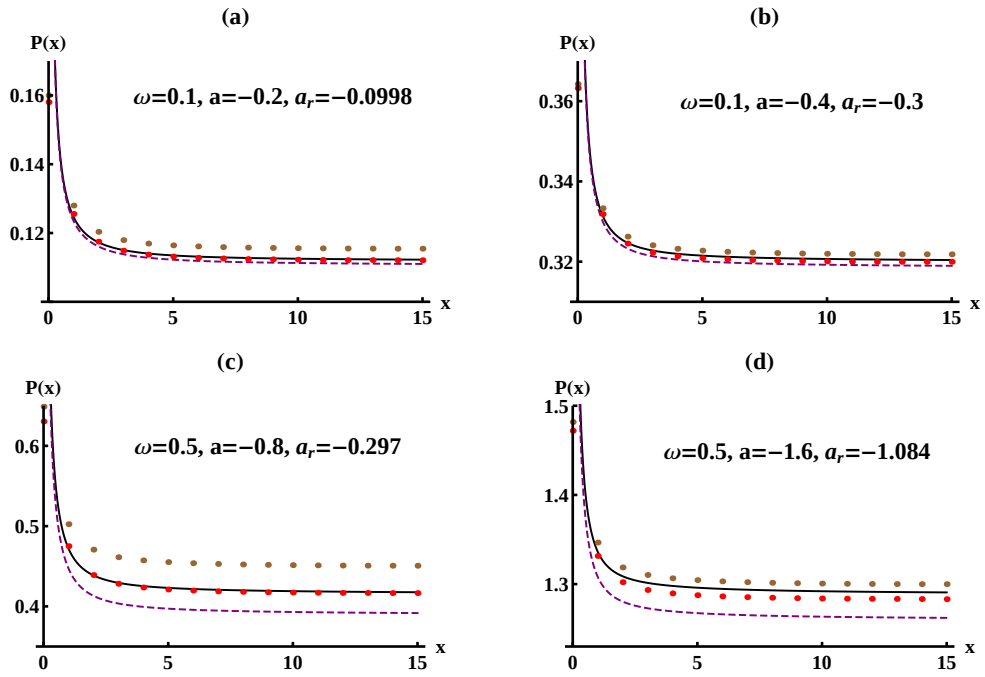

Figure 5: Real space comparison for $P(x)$ in the 3D - $O(2)$ model with different values of ω and a. Black lines are CGA results Eq.(86), and purple dashed lines are perturbation theory up to one loop Eq.(87). The brown dots are one loop results calculated in the lattice model Eq.(89). The red dots are direct Monte Carlo simulations with error bars smaller than the size of points. For each bare parameter a, the corresponding a_r in the continuum model is obtained by the renormalization condition explained in section 4.3.

4. Monte Carlo and CGA calculations of the order parameter correlator

4.1. The CGA calculation of the order parameter correlator

The $O(2)$ invariant order parameter correlator in the symmetry broken phase within CGA is

$$P(\mathbf{k}) = \left\langle \phi^a_{\mathbf{k}} \phi^a_{-\mathbf{k}} \right\rangle = \varphi^2 \delta_{\mathbf{k}} + G^{11}(\mathbf{k}) + G^{22}(\mathbf{k}). \tag{84}$$

The contributions for the full CGA expressions containing the correction are the same as in $d = 1$. The explicit expression for $P(\mathbf{k})$ is rather bulky and is not presented here. The integrals similar to those in 1D were analytically calculated, as shown in Appendix C. For comparison, the perturbation theory starting from an asymmetric classical solution up to one loop, is

$$P_{1loop}(\mathbf{k}) = -a_r \delta_{\mathbf{k}} + \omega \left(\delta_{\mathbf{k}} \frac{3\sqrt{-2a_r}}{4\pi} + \frac{1}{k^2} + \frac{1}{k^2 - 2a_r} \right). \tag{85}$$

The delta function part of order parameter correlator should be included, when we consider the coordinate space counterpart of Eq.(84),

$$P(\mathbf{r}) = \sum\nolimits_{\mathbf{k}} e^{i\mathbf{k}\cdot\mathbf{r}} P(\mathbf{k}) = \varphi^2 + \sum\nolimits_{\mathbf{k}} e^{i\mathbf{k}\cdot\mathbf{r}} \left(G^{11}(\mathbf{k}) + G^{22}(\mathbf{k}) \right). \tag{86}$$

It is compared with the one loop result in the coordinate space,

$$P_{1loop}(\mathbf{r}) = -a_r + \frac{\omega}{4\pi} \left(3\sqrt{-2a_r} + \frac{1 + e^{-\sqrt{-2a_r}|\mathbf{r}|}}{|\mathbf{r}|} \right), \tag{87}$$

in Figure 5, as well as Monte Carlo simulations and perturbation theory on the lattice.

4.2. Monte Carlo simulations of isotropic ϕ^4 model in 3D

To estimate the precision of the CGA, we performed a Monte Carlo simulation of the scalar model on a cubic lattice of size N. The corresponding action is

$$S_L = \frac{1}{\omega}\sum_{\mathbf{i}}\left[\frac{1}{2}\sum_{\alpha}\left(\phi^b_{\mathbf{i}} - \phi^b_{\mathbf{i}-\alpha}\right)^2 + \frac{a}{2}\phi^b_{\mathbf{i}}\phi^b_{\mathbf{i}} + \frac{1}{4}\left(\phi^b_{\mathbf{i}}\phi^b_{\mathbf{i}}\right)^2\right], \tag{88}$$

where $\mathbf{i}$ is the discrete position and α is the unit vector along the three axes. With $O(2)$ symmetry, the summation over $b = 1, 2$ is implicitly assumed. This model has already been precisely simulated by several groups[19, 20] that focused mainly on the critical region. Our interest here is to calculate various quantities in the region of relatively strong thermal fluctuations below the critical point.

The standard Metropolis algorithm is usually inefficient in the broken phase because of the large autocorrelation of the samples. The autocorrelation however can be reduced to a large extent by combining the Metropolis algorithm with the cluster algorithm. This is done by embedding the Ising variables into the Ψ^4 model with $O(2)$ symmetry and using Wolff's single-cluster flipping method[21, 22]. Each cycle of the Monte Carlo iteration contains a single cluster update of the embedded Ising variables, followed by a sweep of local updates of the original fields ϕ^1 and ϕ^2 using Metropolis algorithm. The method was first tested in the free model, that is, without the ϕ^4 terms, for a small sample size $N = 14$. The calculated integrated autocorrelation time was typically less then 10. With such reduced autocorrelation, the statistical error for a run containing several 10^5 cycles after reaching equilibrium is already small enough.

4.3. Comparison with CGA

For measurements sample size of $N = 30$ with periodic boundary condition is used. In order to compare with analytic calculations, the bare parameter a used in the lattice model Eq.(88) has to be related to the renormalized one, a_r, in Eq.(76). The UV cutoff there is, roughly speaking, proportional to the inverse of the lattice distance in a discrete model. While a better way to relate the two parameters is to calculate the same quantity both in the continuum and discrete model, and then compare the results. To this end we use perturbation theory on the lattice. The two point correlator calculated on the lattice,

$$P^L_{\mathbf{i}} = -a + \frac{\omega}{N^3}\sum_{\mathbf{k}}\left(\frac{e^{i\frac{2\pi}{N}\mathbf{k}\cdot\mathbf{i}} - 3}{-2a + 4\sum_i \sin^2\frac{\pi k_i}{N}} + \frac{e^{i\frac{2\pi}{N}\mathbf{k}\cdot\mathbf{i}} - 1}{4\sum_i \sin^2\frac{\pi k_i}{N}}\right), \tag{89}$$

is equated up to order ω with the same quantity calculated in the continuum model Eq.(87) at a particular position, like $(N/2, 0, 0)$.

In Figure 5 the Monte Carlo simulations of the order parameter correlator for $\omega = 0.1$ (relatively small fluctuations) and 0.5 (relatively strong fluctuations) are presented. Two different values of a in the broken phase are given in each case. The red points are MC results, and the black lines are CGA results. The brown dots and purple dashed lines are results of perturbation theory in the lattice and continuum model respectively. One observes that the CGA is much closer to the MC simulations than the perturbation theory in the case of strong fluctuations, which is relevant to high T_c superconductors considered in the next section.

5. Comparison with experiments on penetration depth of high T_c superconductors and discussion

In this section we employ the CGA method to calculate the magnetic penetration depth of a type-II superconductor and compare it with both MC simulations and experiments. Let us first recall the derivation of the magnetic penetration depth within the GL approach.

5.1. Penetration depth of a strongly fluctuating superconductor

Fluctuating magnetic field minimally coupled to the order parameter of a superconductor (represented by a complex field, $\Psi(\mathbf{r}) = \phi^1(\mathbf{r}) + i\phi^2(\mathbf{r})$, in the present context) is contained in the following anisotropic 3D Ginzburg Landau model:

$$F_{GL} = \int_{\mathbf{r}} \left\{ \frac{\hbar^2}{2m^*} \left| \mathbf{D}_{xy} \Psi \right|^2 + \frac{\hbar^2}{2m_c^*} \left| D_z \Psi \right|^2 + \alpha \left(T - T_{mf} \right) |\Psi|^2 + \frac{b}{2} |\Psi|^4 + \frac{(\nabla \times \mathbf{A})^2}{8\pi} \right\}. \tag{90}$$

Here $\mathbf{D} \equiv \nabla + i2\pi\mathbf{A}/\Phi_0$ is the covariant derivative and T_{mf} is the mean - field phase transition temperature. Here we have assumed that the (bare) coefficient of $|\Psi|^2$ is linear in temperature, while other coefficients are temperature independent. This approximation is reasonable in a rather wide range of temperatures around T_c for high temperature superconductors[4].

There are two basic scales, the magnetic penetration depth and the coherence length. The zero temperature magnetic penetration depth is $\lambda_0^2 = \Phi_0^2 m^* b/(4\pi h^2 \alpha T_{mf})$ and together with the *ab*-plane coherence length, $\xi^2 = \hbar^2/(2m^*\alpha T_{mf})$, it defines a dimensionless parameter $\kappa = \lambda_0/\xi$, which is much larger than unity for a typical type-II superconductors. In anisotropic superconductors, like the high T_c cuprates, the ratio $\gamma^2 = m_c^*/m^*$ is large and an additional coherence length scale along the c axis, $\xi_c^2 = \hbar^2/(2m_c^*\alpha T_{mf}) = \xi^2/\gamma^2$, appears. After a scaling of $(x, y, z) \to (\xi x, \xi y, \xi_c z)$, $(A_x, A_y, A_z) \to (\Phi_0/2\pi\kappa)(A_x/\xi, A_y/\xi, A_z/\xi_c)$ and $\Psi \to (T_{mf}\alpha/b)^{1/2}\Psi$, one writes the Boltzmann factor at temperature T as

$$S[\Psi, \mathbf{A}] = \frac{1}{2\omega} \int_{\mathbf{r}} \left\{ \left| \left(\nabla + i\kappa^{-1}\mathbf{A} \right) \Psi \right|^2 + a|\Psi|^2 + \frac{1}{2}|\Psi|^4 \right\} + S_M[\mathbf{A}], \tag{91}$$

where

$$S_M[\mathbf{A}] = \frac{1}{2\omega} \int_{\mathbf{r}} \left\{ \gamma^2 (\nabla \times \mathbf{A})^2 + \left(1 - \gamma^2\right) \left(\partial_x A_y - \partial_y A_x \right)^2 \right\}. \tag{92}$$

Here two dimensionless parameters

$$\omega = \frac{bT}{2\alpha^2 T_{mf}^2 \xi^2 \xi_c} \tag{93}$$

$$a = \frac{T}{T_{mf}} - 1 \tag{94}$$

were introduced. One observes that complexity of the anisotropy is shifted to the kinetic term of the vector field.

To derive mesoscopically the macroscopic electrodynamics of the fluctuating superconductor including the *ab*-plane magnetic penetration depth (or, in the language of field theory the inverse photon mass), one expands the effective action of the photon field to the order of A^2,

$$S_{ind}^{eff}[\mathbf{A}] = \frac{1}{2\omega\kappa^2} \sum_{\mathbf{k}} A_{\mathbf{k}}^{\alpha} A_{-\mathbf{k}}^{\beta} \left[\delta_{\alpha\beta} \sum\nolimits_{\mathbf{q}} \left\langle \left| \Psi_{\mathbf{q}} \right|^2 \right\rangle - \frac{1}{\omega} \left\langle J_{\mathbf{k}}^{\alpha} J_{-\mathbf{k}}^{\beta} \right\rangle_c \right], \tag{95}$$

and then calculates the averages over the order parameter field Ψ within the Ψ^4 isotropic GL model as in the previous sections. For large κ the expression coincides with the leading order in expansion in κ^{-2}. Here

$$J_{\mathbf{k}}^{\alpha} = \frac{1}{2} \sum_{\mathbf{p}} (2\mathbf{p} + \mathbf{k})_{\alpha} \Psi_{\mathbf{p}}^* \Psi_{\mathbf{p}+\mathbf{k}}, \tag{96}$$

is the Noether current density of the $O(2)$ symmetry defined in the pure Ψ^4 model.

Its connected correlator can be decomposed into the transversal and the longitudinal parts,

$$\left\langle J_{\mathbf{k}}^{\alpha} J_{-\mathbf{k}}^{\beta} \right\rangle_c \equiv \left\langle J_{\mathbf{k}}^{\alpha} J_{-\mathbf{k}}^{\beta} \right\rangle - \left\langle J_{\mathbf{k}}^{\alpha} \right\rangle \left\langle J_{-\mathbf{k}}^{\beta} \right\rangle = \chi_T \left(\delta_{\alpha\beta} - \frac{k_\alpha k_\beta}{k^2} \right) + \chi_L \frac{k_\alpha k_\beta}{k^2}. \tag{97}$$

The corresponding coefficient functions, χ_T and χ_L, depend on k^2 only. The term $\sum_{\mathbf{q}} \left\langle |\Psi_{\mathbf{q}}|^2 \right\rangle$ in the effective action Eq.(95) is equal to χ_L/ω due to the "Ward identity" (derived in Appendix D). With this replacement, the induced Boltzmann factor is manifestly gauge invariant and transversal,

$$S_{ind}^{eff}[\mathbf{A}] = \frac{1}{2\omega^2\kappa^2} \sum_{\mathbf{k}} A_{\mathbf{k}}^{\alpha} A_{-\mathbf{k}}^{\beta} \left(\chi_L(k^2) - \chi_T(k^2)\right) \left(\delta_{\alpha\beta} - \frac{k_\alpha k_\beta}{k^2}\right). \tag{98}$$

The magnetic penetration depth for magnetic field along the z direction, $B_k^z = ik_x A_k^y - ik_y A_k^x$, is now derived through the classical equation of motion, i.e. taking derivatives of the effective action with respect to $A_{\mathbf{k}}^{\mu}$. Using the Coulomb gauge, $k_\alpha A_{\mathbf{k}}^{\alpha} = 0$, one obtains

$$0 = \left[k_x^2 + k_y^2 + \gamma^2 k_z^2 + \frac{\chi_L(k^2) - \chi_T(k^2)}{\omega\kappa^2}\right] B_k^z. \tag{99}$$

Therefore the *ab*-plane AC penetration depth in a homogeneous relatively large sample is

$$\frac{\kappa^2}{\lambda^2} = \lim_{k\to 0} \frac{\chi_L(k^2) - \chi_T(k^2)}{\omega}. \tag{100}$$

The remaining work is to calculate the above quantity within the global $O(2)$ GL model.

5.2. CGA calculation of magnetic penetration depth

In this subsection we calculate the penetration depth Eq.(100) using CGA. First let us decompose the order parameter into its real and imaginary parts $\Psi(\mathbf{r}) = \phi^1(\mathbf{r}) + i\phi^2(\mathbf{r})$, so that all the quantities are calculated with CGA in the 3D $O(2)$ model as in previous sections. As explained above the only quantity needed is the current-current correlator that using real fields takes the form:

$$\left\langle J_{\mathbf{k}}^{\alpha} J_{-\mathbf{k}}^{\beta} \right\rangle_c = -\sum_{\mathbf{pq}} (2\mathbf{p} - \mathbf{k})_\alpha (2\mathbf{q} + \mathbf{k})_\beta \left\langle \phi_{\mathbf{k}-\mathbf{p}}^1 \phi_{\mathbf{p}}^2 | \phi_{-\mathbf{k}-\mathbf{q}}^1 \phi_{\mathbf{q}}^2 \right\rangle_c. \tag{101}$$

The notation $\langle AB|CD\rangle_c$ in the above equation means one of A, B should be connected to one of C, D. This quantity therefore contains terms of three and four point connected correlators like $\left\langle \phi_{\mathbf{k}-\mathbf{p}}^1 \phi_{\mathbf{p}}^2 \phi_{-\mathbf{k}-\mathbf{q}}^1 \right\rangle_c$ and $\left\langle \phi_{\mathbf{k}-\mathbf{p}}^1 \phi_{\mathbf{p}}^2 \phi_{-\mathbf{k}-\mathbf{q}}^1 \phi_{\mathbf{q}}^2 \right\rangle_c$. Calculation of these terms requires high order cumulants and within CGA is a combination of the "triangle" and "box" integrals of gaussian truncated Green functions (for an example, see Appendix B, where it was given for the 1D Z_2 model). The calculations of these terms are cumbersome in the 3D case. On the other hand they are believed to give rise to only high order corrections. Therefore we simply ignore all these contributions and approximate the current correlator as

$$\left\langle J_{\mathbf{k}}^{\alpha} J_{-\mathbf{k}}^{\beta} \right\rangle_c = \varphi^2 k_\alpha k_\beta G_{\mathbf{k}}^{22} + \sum\nolimits_{\mathbf{p}} (2\mathbf{p} - \mathbf{k})_\alpha (2\mathbf{p} - \mathbf{k})_\beta G_{\mathbf{k}-\mathbf{p}}^{11} G_{\mathbf{p}}^{22}, \tag{102}$$

where $\left\langle \phi_{\mathbf{k}}^1 \right\rangle = \varphi\delta_{\mathbf{k}}$, $\left\langle \phi_{\mathbf{k}}^2 \right\rangle = 0$ and $G_{\mathbf{k}}^{ab} = \left\langle \phi_{\mathbf{k}}^a \phi_{-\mathbf{k}}^b \right\rangle_c$. With this approximation the penetration depth is given by

$$\frac{\kappa^2}{\lambda^2} = \frac{1}{\omega} \lim_{k\to 0} \left(\frac{3k_\alpha k_\beta}{2k^2} - \frac{\delta_{\alpha\beta}}{2}\right) \left\langle J_{\mathbf{k}}^{\alpha} J_{-\mathbf{k}}^{\beta} \right\rangle_c = \frac{1}{\omega} \lim_{k\to 0} \left[\varphi^2 k^2 G_{\mathbf{k}}^{22} + \sum_{\mathbf{p}} \left(k^2 - 4\mathbf{k}\cdot\mathbf{p} + \frac{6(\mathbf{k}\cdot\mathbf{p})^2}{k^2} - 2p^2\right) G_{\mathbf{k}-\mathbf{p}}^{11} G_{\mathbf{p}}^{22}\right], \tag{103}$$

where the momentum integral in the above equation vanishes in the small k limit.

The magnetic penetration depth calculated this way is therefore proportional to φ^2. Using reasonable values of ω and a_r the above result is in good agreement with MC simulation and the experimental results on various high temperature superconductors.

5.3. Monte Carlo simulation of the penetration depth. Comparison with CGA

The current-current correlator is simulated in the coordinate space for different values of ω and a. In order to compare with the CGA results in the momentum space Eq.(103), finite Fourier transform of the correlators on the lattice is performed. The penetration depth, or the superfluid density, at finite momentum

$$\rho_s(k) \equiv \frac{1}{\omega}\left(\chi_L(k^2) - \chi_T(k^2)\right) \tag{104}$$

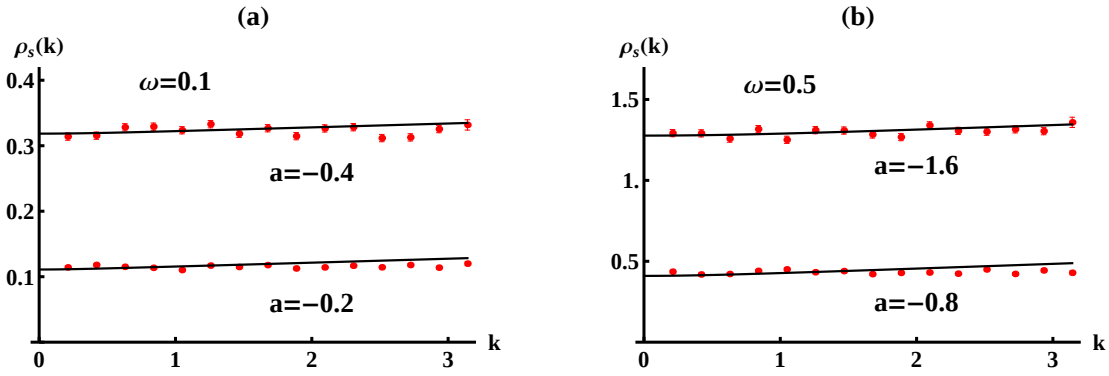

Figure 6: Comparison of finite momentum penetration depth $\rho_s(k)$ for (a) $\omega = 0.1$ and (b) $\omega = 0.5$ between CGA and Monte Carlo calculations. Black lines are CGA results and red dots with error bars are MC results. For each parameter a, the corresponding a_r for the continuum model is the same as that in Figure 5.

is then extracted from the simulated current correlator.

In Figure 6 results of $\rho_s(k)$ at small but finite wave vectors for $\omega = 0.1$ and 0.5 are presented respectively. Red dots with error bars are MC results while black lines are CGA results. Except for the discrepancies at large k, or equivalently small distance between the lattice and continuum model, within the statistical error the two results in small k limit fit well to each other.

5.4. Comparison with experiments on penetration depth of high T_c superconductors

There exists a large amount of experimental data on temperature dependence of magnetic penetration depth in high T_c superconductors. Most effective experimental methods include the microwave surface impedance measurement[10, 11] and the two-coil mutual inductance technique[12, 23]. Both of these two methods determine indirectly the microwave conductivity, $\sigma = \sigma' + i\sigma''$. The superfluid density $\rho_s(T) \propto \lambda^{-2}(T)$ is then extracted from the imaginary part of the conductivity σ''.

In Figure 7a, b, c we compare our CGA results (black lines) with experiments on three different strongly fluctuating high T_c cuprates, optimally-doped bulk materials[10, 11] $Bi_2Sr_2CaCu_2O_8$, $Tl_2Ba_2CuO_{6+y}$, and $YBa_2Cu_3O_{7-\delta}$ thin film with a thickness of 10 unit cells[12], respectively. The dimensionless ratio, $\lambda^2_{ab}(0)/\lambda^2_{ab}(T)$, is shown within about one third of the whole temperature range below T_c, where the GL model with linear temperature dependence of the bare coefficient a Eq.(94) is still applicable. Straight dashed lines in Figure 7 are mean-field approximation of the corresponding material. At lower temperatures it is tangential to both CGA and experimental data. The estimated mean field critical temperature T_{mf} is the intersection point between the dashed line and the T axis. One observes that renormalization of T_{mf} to T_c given in gaussian approximation by Eq.(76)

$$T_c = T_{mf}\left(1 - \frac{2\omega T_{mf}\Lambda\xi}{\pi^2 T}\right), \tag{105}$$

compares reasonably well with experiments for value of UV momentum cutoff of order $\Lambda = 0.25/\xi$, deduced from the fluctuation diamagnetism[14] for somewhat different materials.

Another feature is the downward curvature of the inverse magnetic penetration depth within a temperature range below the critical point that is much wider than the critical region. This is possibly a non - universal phenomenon caused by strong thermal fluctuations. Given experimentally measured critical temperature T_c, the dimensionless thermal fluctuation strength parameter ω ($\omega T_c/T$, proportional to the square root of Ginzburg number Gi) is the only parameter used to fit the experimental data. For $Bi_2Sr_2CaCu_2O_8$ the resulting value is $\omega = 1$ (corresponding to $Gi = 0.013$), while for $YBa_2Cu_3O_{7-\delta}$ and $Tl_2Ba_2CuO_{6+y}$ one gets $\omega = 0.5$ ($Gi = 0.0032$) and $\omega = 0.54$ ($Gi = 0.0037$) respectively.

One observes that the downward cusp, while absent in the mean field result is described reasonably well by CGA. Note however that all the three materials are marginally three dimensional, and the use of the anisotropic 3D GL,

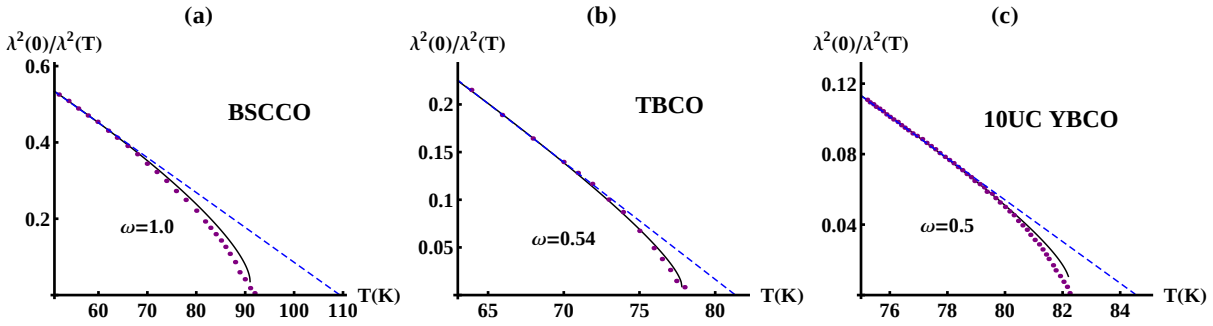

Figure 7: Comparison of experimentally measured magnetic penetration depth in (a) BSCCO, (b) TBCO, and (c) 10 unit cells YBCO with CGA calculations. The purple dots are experimental data. The black lines are CGA results. The blue dashed lines are the corresponding mean field behaviors.

Eq.(90), for these highly anisotropic materials is justified since the coherence length in the c direction (perpendicular to the CuO planes) exceeds the layer spacing. Perhaps the Lawrence - Doniach model can give an improved description. Width of the sample even for the 10 unit cells (each containing a bilayer of the CuO planes) $YBCO$ is still large enough to neglect the finite size effect. It is not clear whether the Kosterlitz - Thouless transition takes place. Generalizing the CGA method to 2D or layered superconductors to describe the 2D-3D crossover is beyond the scope of the present paper.

6. Conclusions

To summarize, we have developed a non - perturbative method to account for the strong thermal fluctuations within phenomenological Ginzburg - Landau approach. The approximation can be broadly described as a systematic correction of the Hartree - Fock type of mean field description of condensed matter systems undergoing second order transition. The correction to any correlator (one or two - body considered in the paper) makes the approximation "covariant", i. e. it obeys all the Ward identities of the relevant symmetry. The development of such an improvement scheme is motivated by recent experimental realization (in magnetization, conductivity and Nernst effect) that the fluctuation effects are strong in a much wider region both above and below T_c than the narrow (even in high T_c superconductors) critical fluctuation region (determined by the Ginzburg criterion, $|T/T_c - 1| \ll Gi$), and the theoretical requirement of a conserving approximation for calculating quantities that hinge on the symmetry like the magnetic penetration depth in superconductors.

We have demonstrated how all the physical consequences of the symmetry like the Goldstone theorem and gauge invariance of the current correlator (that enters the calculation of the magnetic penetration depth) are restored in the CGA. The method was tested on solvable one - dimensional models and by comparison with direct Monte Carlo simulation of realistic 3D model. It turns out that the covariant gaussian approximation captures correctly the excitation branches in addition to the modes described by the mean field approximation. This is clearly demonstrated by calculation of the four - field correlators in a toy model.

We have performed the Monte Carlo simulations of the magnetic penetration depth in the symmetry broken phase of the 3D Ginzburg - Landau model. It compares well with CGA in the range accessible for the MC evaluation. The experimental measurements of the temperature dependence of penetration depth in high T_c cuprates including the downward curvature induced by strong fluctuations is well captured by the CGA calculations.

Recently it has been demonstrated that several new monolayer 2D materials like $FeSe$ on STO substrate[24] to be superconducting. The high critical temperature and low dimensionality ensures strong thermal fluctuations. The corresponding superconducting transition of these 2D materials can be of the Kosterlitz-Thouless type[1]. It would be interesting to apply the CGA approach to the two - dimensional GL model. It is not straightforward to describe KT phase transitions, since the $O(2)$ symmetric toy model considered in the present paper demonstrates there are infrared divergencies[25], and it will be considered in a later work. The method can be generalized to time dependent Ginzburg - Landau equations and to the many - body system in which quantum fluctuations are included on the mesoscopic scale.

Then the discussion of the fluctuations effects in transport can be quantitatively addressed. Moreover, it is well known that strong magnetic field enhances the thermal fluctuations, and magnetic field and vortex physics can also be easily incorporated using the CGA.

Acknowledgment

Authors are very grateful to B. Shapiro and R.C Ma for numerous discussions. H. Kao and B. Rosenstein were supported by MOST of Taiwan through Contract Grant 104-2112-M-003-012, and 103-2112-M-009-009-MY3. J.F. Wang and D.P. Li were supported by National Natural Science Foundation of China (No. 11274018 and No. 11674007). B.R. is grateful to School of Physics of Peking University and Bar Ilan Center for Superconductivity for hospitality.

Appendix A. Calculation of the invariant correlators in d=1 (Quantum Mechanics)

We use the numerical diagonalization of the quantum mechanics to compute the correlators. The correlator after renaming $\phi(x)$ of statistical physics by $x(t)$ of Euclidean quantum mechanics (t being the Matsubara time) is

$$P(t) = \Theta(t)\left\langle 0\left|e^{tH}xe^{-tH}x\right|0\right\rangle + \Theta(-t)\left\langle 0\left|xe^{tH}xe^{-tH}\right|0\right\rangle, \tag{A.1}$$

where $\Theta(t)$ is the step function and the Hamiltonian of the double well is

$$H = -\frac{1}{2}\partial^2 + \frac{a}{2}x^2 + \frac{1}{4}x^4. \tag{A.2}$$

Sandwiching the full set of eigenstates, one obtains

$$P(t) = \sum\nolimits_{n>0} |\langle 0|x|n\rangle|^2 \left\{\Theta(t)\, e^{-(E_n-E_0)t} + \Theta(-t)\, e^{(E_n-E_0)t}\right\}; \tag{A.3}$$

$$P(\omega) = |\langle 0|x|0\rangle|^2\, 2\pi\delta(\omega) + \sum\nolimits_{n>0} |\langle 0|x|n\rangle|^2 \frac{2(E_n-E_0)}{\omega^2 + (E_n-E_0)^2}. \tag{A.4}$$

In particular $P(\omega=0) = 2\left\langle\left|x\frac{1}{H-E_0}x\right|\right\rangle$. These may be easily calculated numerically and presented in Figure 1 (as a function of Matsubara time) and Figure 2 (as a function of frequency).

Appendix B. Correlator of composite operator $\phi^2(r)$ in the 1D Z_2 model

In section 2 we have derived the two - point cumulant $\Gamma(x,y)$ within the CGA by taking derivative of the shift equation with respect to $\varphi(r)$. Similarly, one can derive higher order cumulants by taking more and more derivatives, for example, the three - point cumulant is (again we set $\omega = 1$),

$$\Gamma_3(z,x,y) = \frac{\delta\Gamma(x,y)}{\delta\varphi(z)} = 3\left[2\varphi(x)\delta(x-y) + C(y|x,x)\right]\delta(x-z) + 3C(z|x,x)\delta(x-y) + 3\varphi(x)\, C_4(y,z|x,x). \tag{B.1}$$

Therefore the function,

$$C_4(y,z|x,x') \equiv \frac{\delta^2 G^{tr}(x,x')}{\delta\varphi(z)\,\delta\varphi(y)} = \frac{\delta C(y|x,x')}{\delta\varphi(z)}, \tag{B.2}$$

is the only new unknown chain function that we have to calculate. Performing the functional derivative of Eq.(43), one obtains:

$$\begin{aligned} C_4(y,z|x,x') = & -\int_{u,v} C(z|x,u)\Gamma_3^{tr}(y,u,v)G^{tr}(v,x') - \int_{u,v} G^{tr}(x,u)\Gamma_3^{tr}(y,u,v)C(z|v,x') \\ & - \int_{u,v} G^{tr}(x,u)\Gamma_4^{tr}(y,z,u,v)G^{tr}(v,x'). \end{aligned} \tag{B.3}$$

Here again the superscript "tr" of Γ_3^{tr} and Γ_4^{tr} indicates they are derivatives of the truncated gap equation Eq.(38), i.e.,

$$\Gamma_3^{tr}(y,u,v) = \left[6\varphi(u)\,\delta(u-y) + 3C(y|u,u)\right]\delta(u-v), \tag{B.4}$$

and

$$\Gamma_4^{tr}(y,z,u,v) = 6\delta(u-z)\delta(u-y)\delta(u-v) + 3C_4(y,z|u,u)\delta(u-v). \tag{B.5}$$

Substituting Eq.(B.4) and Eq.(B.5) into Eq.(B.3), after some rearrangements one finally gets

$$C_4(y,z|x,x') + 3\int_u G^{tr}(x,u)G^{tr}(u,x')C_4(y,z|u,u) = \cdots \tag{B.6}$$

where "$\cdots$" contains all the terms we have already encountered in section 2. This chain equation for C_4 is analogous to Eq.(45). We need only the particular case for $x = x'$. Using the translation invariance, it can be easily solved in the momentum space:

$$c_{p,q}^4 = \frac{6\left[12\varphi^2 t_{p,q} - f_q\left(1+3f_{-p}\right)\left(1+3f_{p+q}\right)\right]}{\left(1+3f_{-p}\right)\left(1+3f_q\right)\left(1+3f_{p+q}\right)}. \tag{B.7}$$

Here the Fourier transform is defined as

$$C_4(y,z|x,x) = \int_{p,q} c_{p,q}^4 e^{ip(y-z)}e^{iq(y-x)}, \tag{B.8}$$

and $t_{p,q}$ is the "triangle" integral

$$t_{p,q} = \sum\nolimits_k g_k^{tr} g_{p-k}^{tr} g_{q+k}^{tr}. \tag{B.9}$$

Substituting Eq.(B.7) and Eq.(51) into the Fourier form of Eq.(B.1), one gets the final expression for Γ_3:

$$\Gamma_{p,q}^3 = 6\varphi + 3\left(c_{p+q} + c_{-q} + \varphi c_{p,q}^4\right). \tag{B.10}$$

The derivation of Γ_4 is similar but far more complicated. Except for the above mentioned chain functions, one would also need a higher order chain,

$$C_5(y,z,u|x,x) \equiv \frac{\delta^2 G^{tr}(x,x)}{\delta\varphi(y)\,\delta\varphi(z)\,\delta\varphi(u)} = \int_{p,q,k} c_{p,q,k}^5 e^{ip(y-z)}e^{iq(y-u)}e^{ik(y-x)}, \tag{B.11}$$

which is a complicated function of "fish", "triangle" and even "box" integrals,

$$b_{p,q,k} = \sum\nolimits_l g_l^{tr} g_{p+l}^{tr} g_{p+q+l}^{tr} g_{p+q+k+l}^{tr}. \tag{B.12}$$

The expression in terms of these integrals is rather bulky and will not be presented here. The final expression for Γ_4 in terms of chain functions is

$$\Gamma_{p,q,k}^4 = 6 + 3\left(c_{k,p+q}^4 + c_{k,-p-k}^4 + c_{p,q+k}^4 + 3\varphi c_{p,k,q}^5\right). \tag{B.13}$$

Combining all these building blocks, one is able to calculate the composite operator correlator

$$\begin{aligned} P_2(k) &\equiv \int_x e^{-ikx}\left\langle\phi(x)^2\,\phi(0)^2\right\rangle = \sum_{pq}\left\langle\phi_p\phi_{k-p}\phi_q\phi_{-k-q}\right\rangle \\ &= C\delta_k + 4\varphi^2\left\langle\phi_k\phi_{-k}\right\rangle_c + 2\sum_p\left\langle\phi_{k-p}\phi_{p-k}\right\rangle_c\left\langle\phi_p\phi_{-p}\right\rangle_c + 4\varphi\sum_p\left\langle\phi_p\phi_{k-p}\phi_{-k}\right\rangle_c + \sum_{pq}\left\langle\phi_p\phi_{k-p}\phi_q\phi_{-k-q}\right\rangle_c. \end{aligned} \tag{B.14}$$

The delta function part comes from disconnected diagrams and the three and four - point connected correlation functions can be expressed via the two - point connected correlator and the cumulants derived above. The results for $k \neq 0$ (that arise from the "would be" broken phase solution of the minimization equations) and that arise from the symmetric one are compared in Figure 4 with the exact result of numerical diagonalization.

Appendix C. Solution of minimization equations in the O (2) d=3 model

Appendix C.1. The "fish" integral for the O (2) d=3 model

The result of fish integral Eq.(80) in 3D is:

$$f_k^{ab} = \frac{1}{8\pi k}\left[\arcsin\frac{k^2+m_a^2-m_b^2}{\sqrt{\left(k^2-m_a^2+m_b^2\right)^2+4k^2m_a^2}} - \arcsin\frac{-k^2+m_a^2-m_b^2}{\sqrt{\left(k^2-m_a^2+m_b^2\right)^2+4k^2m_a^2}}\right]. \tag{C.1}$$

In particular, one gets in the limit of $k \to 0$:

$$f_0^{ab} = \frac{1}{4\pi\left(m_a+m_b\right)}. \tag{C.2}$$

Appendix C.2. Solution of minimization equations for the O (2) d=3 model

The minimization equations for the broken phase $\varphi \neq 0$ are

$$0 = a_r + \varphi^2 - \frac{3\omega}{4\pi}m_1 - \frac{\omega}{4\pi}m_2; \tag{C.3}$$

$$m_1^2 = a_r + 3\varphi^2 - \frac{3\omega}{4\pi}m_1 - \frac{\omega}{4\pi}m_2; \tag{C.4}$$

$$m_2^2 = a_r + \varphi^2 - \frac{\omega}{4\pi}m_1 - \frac{3\omega}{4\pi}m_2. \tag{C.5}$$

The first two equations give us

$$m_1^2 = 2\varphi^2 = \left(\frac{2\pi}{\omega}m_2^2 + m_2\right)^2. \tag{C.6}$$

Substituting this into Eq.(C.5) one has

$$a_r = \frac{-2\pi^3m_2^4 - 2\pi^2\omega m_2^3 + \pi\omega^2m_2^2 + \omega^3m_2}{\pi\omega^2} \tag{C.7}$$

The right hand side of the above equation has a maximum of $0.03935\omega^2$, above which there is no solution. Therefore the line $a_r(\omega) = 0.03935\omega^2$ is the boundary of the symmetry broken solution in the $a_r \sim \omega$ phase diagram. The quartic equation Eq.(C.7) does not uniquely determine m_2 in terms of a_r. One requires additional conditions, $m_2 > 0$ and $\partial a_r/\partial m_2 \leq 0$. Since for this branch the "Higgs" excitation within the CGA is

$$m_H^2 = m_1^2 + \Delta\Gamma_{k=0}^{11} = \frac{2\pi\omega m_1^2}{8\pi^2m_1m_2 + 3\pi\omega\left(m_1+m_2\right)+\omega}\frac{-\partial a_r}{\partial m_2}, \tag{C.8}$$

the conditions are necessary for positivity of m_H^2. Consistently the boundary of symmetry broken phase is specified by $\partial a_r/\partial m_2 = 0$.

For the symmetric phase $\varphi = 0$, the minimization equations reduce to,

$$m_1^2 = m_2^2 \equiv m^2 = a_r - \frac{\omega}{\pi}m, \tag{C.9}$$

giving rise to the solution

$$m = \frac{1}{2\pi}\left(\sqrt{\omega^2+4\pi^2a_r}-\omega\right). \tag{C.10}$$

It exists for any $a_r > 0$. Therefore in the small region $0 < a_r < 0.03935\omega^2$ both the symmetric and asymmetric solutions exist.

Appendix D. Proof of Ward Identity for the current correlator

The partition function,

$$Z \equiv \int \mathcal{D}\Psi e^{-S} = \int \mathcal{D}\Psi \exp\left[-\frac{1}{\omega}\int_{\mathbf{r}}\left\{\frac{1}{2}\left|\nabla\Psi\right|^2 + \frac{a}{2}\left|\Psi\right|^2 + \frac{1}{4}\left|\Psi\right|^4\right\}\right], \tag{D.1}$$

is invariant under the local unitary transformation

$$\Psi(\mathbf{r}) \to \Psi(\mathbf{r})e^{i\theta(\mathbf{r})}. \tag{D.2}$$

The measure $\mathcal{D}\Psi$ is invariant under this transformation. This gives

$$Z = \int \mathcal{D}\Psi \exp\left[-\frac{1}{\omega}\int_{\mathbf{r}}\left(\mathbf{J} + \frac{1}{2}\left|\Psi\right|^2\nabla\theta\right)\cdot\nabla\theta\right]e^{-S}. \tag{D.3}$$

For small $\nabla\theta$ the integrand in the above equation can be expanded to the second order of $\nabla\theta$:

$$1 - \frac{1}{\omega}\int_{\mathbf{r}}\mathbf{J}\cdot\nabla\theta - \frac{1}{2\omega}\int_{\mathbf{r}}\left|\Psi\right|^2(\nabla\theta)^2 + \frac{1}{2\omega^2}\int_{\mathbf{r},\mathbf{r}'}(\mathbf{J}\cdot\nabla\theta)_{\mathbf{r}}(\mathbf{J}\cdot\nabla\theta)_{\mathbf{r}'}. \tag{D.4}$$

Due to the invariance of Z, linear and quadratic terms in θ vanish:

$$\nabla\cdot\langle\mathbf{J}\rangle = 0; \tag{D.5}$$

$$\partial^{\alpha}_{\mathbf{r}}\partial^{\beta}_{\mathbf{r}'}\left(\frac{1}{\omega}\left\langle\mathbf{J}^{\alpha}_{\mathbf{r}}\mathbf{J}^{\beta}_{\mathbf{r}'}\right\rangle - \left\langle\left|\Psi_{\mathbf{r}}\right|^2\right\rangle\delta_{\alpha\beta}\delta(\mathbf{r}-\mathbf{r}')\right) = 0. \tag{D.6}$$

The Fourier transform of the second equation leads to the following "Ward Identity":

$$0 = k^{\alpha}k^{\beta}\left[\frac{1}{\omega}\left\langle J^{\alpha}_{\mathbf{k}}J^{\beta}_{-\mathbf{k}}\right\rangle - \sum\nolimits_{\mathbf{q}}\left\langle\left|\Psi_{\mathbf{q}}\right|^2\right\rangle\delta_{\alpha\beta}\right] = k^2\left[\frac{1}{\omega}\chi_L(k^2) - \sum\nolimits_{\mathbf{q}}\left\langle\left|\Psi_{\mathbf{q}}\right|^2\right\rangle\right]. \tag{D.7}$$

References

[1] P.M. Chaikin and T.C. Lubensky, Principles of condensed matter physics, Campridge University Press, 1995.
[2] D.J. Amit, Field Theory, the Renormalization Group, and Critical Phenomena, World Scientific, 1984.
[3] A. Larkin and A. Varlamov, Theory of fluctuations in superconductors, Clarendon Press, Oxford, 2005.
[4] B. Rosenstein and D.P. Li, Rev. Mod. Phys. 82 (2010) 109.
[5] D.P. Li and B. Rosenstein, Phys. Rev. B 60 (1999) 9704.
[6] M. Tinkham, Introduction to Superconductivity, McGraw-Hill, Inc., 1996.
[7] L. Li, Y. Wang, S. Komiya, S. Ono, Y. Ando, G.D. Gu, and N.P. Ong, Phys. Rev. B 81 (2010) 054510; Y. Wang, L. Li, M.J. Naughton, G.D. Gu, S. Uchida, and N.P. Ong, Phys. Rev. Lett. 95 (2005) 247002.
[8] F. Rullier-Albenque, H. Alloul, and G. Rikken, Phys. Rev. B 84 (2011) 014522 and references therein; M.S. Grbic, M. Pozek, D. Paar, V. Hinkov, M. Raichle, D. Haug, B. Keimer, N. Barisic, and A. Dulcic, Phys. Rev. B 83 (2011) 144508.
[9] Z.A. Xu, N.P. Ong, Y. Wang, T. Kakeshita and S. Uchida, Nature 406 (2000) 486; Y. Wang, Z.A. Xu, T. Kakeshita, S. Uchida, S. Ono, Y. Ando, and N.P. Ong, Phys. Rev. B 64 (2001) 224519; Y. Wang, N.P. Ong, Z.A. Xu, T. Kakeshita, S. Uchida, D.A. Bonn, R. Liang, and W.N. Hardy, Phys. Rev. Lett. 88 (2002) 257003.
[10] S.F. Lee, D.C. Morgan, R.J. Ormeno, D.M. Broun, R.A. Doyle, and J.R. Waldram, Phys. Rev. Lett. 77 (1996) 735.
[11] D.M. Broun, D.C. Morgan, R.J. Ormeno, S.F. Lee, A.W. Tyler, A.P. Mackenzie, and J.R. Waldram, Phys. Rev. B 56 (1997) R11443.
[12] Y. Zuev, J.A. Skinta, M.S. Kim, T.R. Lemberger, E. Wertz, K. Wu, and Q. Li, 2004. arXiv: cond-mat/0407113.
[13] A.L. Solovev and V.M. Dmitriev, Low Temperature Physics 35 (2009) 169; T. Timusk and B. Statt, Rep. Prog. Phys. 62 (1999) 61; P.A. Lee, N. Nagaosa, and X.G. Wen, Rev. Mod. Phys. 78 (2006) 17.
[14] X.J. Jiang, D.P. Li, and B. Rosenstein, Phys. Rev. B 89 (2014) 064507.
[15] P.M. Stevenson, Phys. Rev. D 23 (1981) 2916.
[16] G. Baym and L.P. Kadanoff, Phys. Rev. 124 (1961) 287; T. Kita, Phys. Rev. B 80 (2009) 214502; F. Cooper, C.-C. Chien, B. Mihaila, J. F. Dawson, and E. Timmermans, Phys. Rev. Lett. 105 (2010) 240402.
[17] A. Kovner and B. Rosenstein, Phys. Rev. D 39 (1989) 2332; A. Kovner and B. Rosenstein, Phys. Rev. D 40 (1989) 504.
[18] J.M. Cornwall, R. Jackiw, and E. Tomboulis, Phys. Rev. D 10 (1974) 2428.
[19] P. Arnold and G.D. Moore, Phys. Rev. E 64 (2001) 066113.
[20] M. Hasenbusch and T. Torok, Journal of Physics A: Mathematical and General 32 (1999) 6361.

[21] R.C. Brower, P. Tamayo, Phys. Rev. Lett. 62 (1989) 1087.
[22] U. Wolff, Phys. Rev. Lett. 62 (1989) 361; U. Wolff, Phys. Lett. B 228 (1989) 379.
[23] A.T. Fiory, A.F. Hebard, P.M. Mankiewich, and R.E. Howard, Appl. Phys. Lett. 52 (1988) 2165.
[24] Q.Y. Wang, Z. Li, W.H. Zhang, Z.C. Zhang, J.S. Zhang, W. Li, H. Ding, Y.B. Ou, P. Deng, and K. Chang, Chin. Phys. Lett. 29 (2012) 037402; Y. Sun, W.H. Zhang, Y. Xing, F.S. Li, Y.F. Zhao, Z.C. Xia, L.L. Wang, X.C. Ma, Q.K. Xue, and J. Wang, Scientific reports 4 (2014); J.F. Ge, Z.L. Liu, C.H. Liu, C.L. Gao, D. Qian, Q.K. Xue, Y. Liu, and J.F. Jia, Nature materials 14 (2015) 285.
[25] H.C. Kao, B. Rosenstein and J.C. Lee, Phys. Rev. B 61 (2000) 12352.